Topology of surface diagrams of smooth 4-manifolds

Jonathan D. Williams[1]

Department of Mathematics, University of California, Berkeley, CA 94720-3840

Edited* by Robion C. Kirby, University of California, Berkeley, CA, and approved March 2, 2011 (received for review December 3, 2010)

Surface diagrams are a new way to specify any smooth closed orientable 4-manifold by an orientable surface decorated with simple closed curves. These curves are cyclically indexed, and each curve has a unique transverse intersection with the next. The aim of this paper is to announce a uniqueness theorem for these objects (within a fixed homotopy class) that turns out to be similar to the Reidemeister-Singer theorem for Heegaard splittings of 3-manifolds.

broken | Lefschetz fibration

The purpose of this paper is to continue the development of objects called broken Lefschetz fibrations in a topological direction with a theorem that relates those fibrations within a constricted (yet suitably large) class, called simplified purely wrinkled fibrations. The result involves certain moves, called stabilization, handleslide, shift, and multislide, that can be performed within the class of surface diagrams for a fixed 4-manifold.

Theorem 1. *Suppose* $\alpha_0,\alpha_1\colon M \to S^2$ *are two homotopic simplified purely wrinkled fibrations. Then their corresponding surface diagrams become diffeomorphic after some finite sequence of stabilizations, handleslides, shifts, and multislides. When* M *is simply connected, the sequence can be assumed to be free of multislides.*

Background

This section outlines the origins and motivation for broken Lefschetz fibrations and surface diagrams, and its content should be accessible to mathematicians with some topological background. The exposition that explains the vocabulary of Theorem 1 begins in the next section and should be accessible to a wider audience.

Broken Lefschetz fibrations on smooth 4-manifolds were first introduced in ref. 1 to generalize the correspondence between Lefschetz fibrations and symplectic 4-manifolds up to blowup. A symplectic form on a 4-manifold M is a closed two-form ω whose square is a volume form at every point of M. Given such a two-form, and possibly after blowing up M at a finite number of points, the resulting symplectic 4-manifold admits a compatible Lefschetz fibration, which is a surface bundle over a surface, except that it is allowed to have a discrete collection of so-called Lefschetz critical points, locally modeled in complex coordinates by $(z,w) \mapsto zw$. In the above correspondence, ω restricts to a volume form on each fiber (see section 10.2 of ref. 2 for further details on symplectic structures and Lefschetz fibrations). Roughly, the result of ref. 1 was that if one allows ω to vanish in a controlled way along an embedded one-submanifold of M [that is, (M,ω) is a near-symplectic 4-manifold], then a suitable blowup of (M,ω) has a *broken* Lefschetz fibration such that, away from its vanishing locus, ω restricts to a volume form on the fiber. Discussed below, broken Lefschetz fibrations are a mild generalization of Lefschetz fibrations in which the critical locus is allowed to contain a one-submanifold of critical points; when the fibration corresponds to a near-symplectic form, this critical one-submanifold coincides with its vanishing locus (see, for example, refs. 3 and 4). Though mild, this generalization greatly increases the collection of 4-manifolds that admit such a fibration structure: It is known that *every* smooth, orientable 4-manifold admits a broken Lefschetz fibration (though it may not correspond to any near-symplectic form); see, for example, refs. 4–6.

The study of broken Lefschetz fibrations is partly motivated by the effort to understand the Seiberg–Witten invariant of a smooth 4-manifold M geometrically. The Seiberg–Witten invariant is a gauge-theoretic invariant defined as a count of solutions to an elliptic pair of partial differential equations whose input consists of a spin^C structure (equipped with a connection on its determinant line bundle) on the tangent space of M. In a 1996 paper, Taubes showed that, for symplectic 4-manifolds, solutions to the Seiberg–Witten equations correspond to pseudoholomorphic curves which contribute to a special Gromov invariant he defined, called Gr. Pseudoholomorphic curves are submanifolds of two real dimensions that are singled out by the chosen symplectic structure and other auxiliary data (these are choices which are later shown to not affect the values of Gr) (7).

Recent efforts to geometrically recover Seiberg–Witten theory for 3-manifolds and more general 4-manifolds have revolved around equipping a given manifold with structures that resemble surface bundles, namely Morse functions in three dimensions and (broken) Lefschetz fibrations in four dimensions. An initial development in the latter case appeared in a 2003 paper in which Donaldson and Smith defined a *standard surface count* for symplectic 4-manifolds, counting pseudoholomorphic curves which are sections of a fiber bundle associated to a Lefschetz fibration (8). For the standard surface count, these so-called multisections can be realized as pseudoholomorphic curves in M on which the fibration restricts to a branched cover over the sphere: Generically, a fiber intersects a multisection positively at k points, where $k > 0$ does not depend on the chosen fiber. In this sense, a multisection locally resembles k distinct sections of the fibration, but it is actually a single "section" that wraps around the total space k times. Soon after the appearance of this work, Usher showed that the standard surface count is equivalent to Gr, and thus the Seiberg–Witten invariant (9). Though this equivalence is only known to hold for a suitably chosen Lefschetz fibration whose existence is equivalent to the existence of a symplectic form, it gave a promising inroad to generalization by looking at more general fibration structures: Broken Lefschetz fibrations offer a way to continue their approach into nonsymplectic territory, further guided by an existence result of ref. 10, stating that if a near-symplectic 4-manifold has nonvanishing Seiberg–Witten invariant, then there is a pseudoholomorphic subvariety with boundary given by the vanishing locus of ω.

In a 2007 paper, Perutz defined a generalization of the standard surface count for near-symplectic broken Lefschetz fibrations, called the *Lagrangian matching invariant*, in which the multisections are defined over regions in the base of the fibration (11). These regions are defined by removing an immersed collection of circles, the image of the vanishing locus of ω, from the base. Over each region, the map is a symplectic Lefschetz fibration mapping to a surface with boundary, with the parameter k depending on the genus of the fiber over each region. The multisections over adjacent regions are then glued together using data

Author contributions: J.D.W. designed research, performed research, and wrote the paper.

The author declares no conflict of interest.

*This Direct Submission article had a prearranged editor.

[1]E-mail: jdw@math.berkeley.edu.

coming from the fibration over the places where the regions meet. It turns out that k changes by one when moving between adjacent regions, leading to the patched-together multisection having boundary; this boundary must meet certain conditions, again coming from the fibration structure where the regions meet. The Lagrangian matching invariant fits in nicely with experts' expectations and ref. 10 in numerous ways. For example, there are formal similarities, vanishing theorems and calculations in special cases that coincide with those for the Seiberg–Witten invariant. However, it remains to show that the Lagrangian matching invariant is a smooth invariant of the underlying 4-manifold (not just the isomorphism class of the chosen fibration structure), and it is generally difficult to compute. A large amount of the motivation for studying surface diagrams is the possibility that they will prove useful in addressing this pair of issues.

Aside from these speculative applications, one aspect of surface diagrams which (depending on one's perspective) may be taken as a strength is that there are surface diagrams for each smooth, closed orientable 4-manifold. Of particular interest is that a surface diagram is a combinatorial object in the same sense as Heegaard diagrams for 3-manifolds. Considering how fruitful Heegaard diagrams have been in the study of 3-manifolds, a specific goal would be a combinatorially defined and calculated smooth 4-manifold invariant: Through surface diagrams, the complicated three-dimensional nature of handlebody theory on 4-manifolds has been transferred to the combinatorics of a collection of circles on a surface.

Fibration Structures and Critical Points

In this section, we define the fibration structures mentioned above and describe ways of recording them: A convenient way to specify a fibration structure when one only cares about smooth phenomena (as opposed to complex or symplectic) is to restrict the critical locus of the underlying map, and this is our approach. Let M be a smooth closed 4-manifold. A generic map $M \to S^2$ resembles a surface bundle, except one allows the presence of a one-dimensional critical locus that is a union of *fold* and *cusp* points. The collection of fold points forms an embedded one-submanifold of M with the following local model at each point:

$$(x_1,x_2,x_3,x_4) \mapsto (x_1,x_2^2+x_3^2 \pm x_4^2). \qquad [1]$$

When the sign above is negative, it is known variously as an indefinite fold, round singularity, or broken singularity depending on context. Fig. 1*A* is a base diagram for the indefinite fold: It is a picture of the target space for this map and its fibration structure. In that figure, like the one to its right, what appears is the target disk of a map $D^4 \to D^2$, with bold arcs representing the image of the critical locus. A surface is pictured in the region of regular values that have that surface as their preimage, so that, for example, the fibers above points to the left of the vertical arc in Fig. 1*A* are cylinders and to the right they are pairs of disks. In Fig. 1*A*, tracing point preimages above a horizontal arc from left to right gives the foliation of $\mathbb{R}^3$ by hyperboloids, first one-sheeted, then two-sheeted, with a double cone above each point in the vertical arc. The circle (drawn on the cylinder to the left) that shrinks to the cone point is called the round vanishing cycle for that arc in the context of broken Lefschetz fibrations. When dealing with purely wrinkled fibrations, those whose critical locus consists only of indefinite folds and indefinite cusps (described below), there are no Lefschetz vanishing cycles, so the term "vanishing cycle" will suffice in that case.

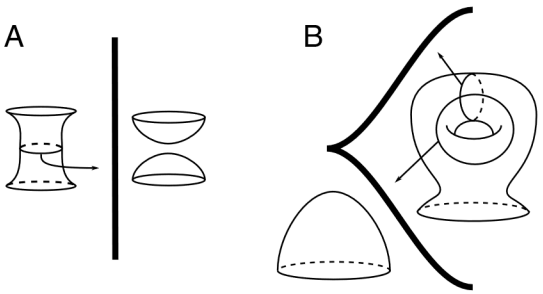

Fig. 1. Critical points of purely wrinkled fibrations: (*A*) fold, (*B*) cusp.

Each cusp point is a common endpoint of two open arcs of fold points, with the local model

$$(x_1,x_2,x_3,x_4) \mapsto (x_1,x_2^3-3x_1x_2+x_3^2 \pm x_4^2). \qquad [2]$$

When the sign above is negative, it is called an indefinite cusp and it is a common endpoint of two indefinite fold arcs as in Fig. 1*B*: Here, two fold arcs meet at a cusp point, for which the two vanishing cycles must intersect at a unique point in the fiber. These two local models (with the preferred signs) are a proper subset of the possible critical loci available to generic maps from 4- to 2-manifolds, and there is an even greater variety when one considers one-parameter families of such maps: For full details on genericity and critical loci, see refs. 12 and 13.

Conspicuously absent from this paper is an actual broken Lefschetz fibration. Topologically, such an object is a smooth map from a 4-manifold to a 2-manifold whose critical locus consists of Lefschetz critical points and indefinite folds. Results from ref. 4 imply that purely wrinkled fibrations and broken Lefschetz fibrations are interchangeable by small homotopies, so that in the course of study or exposition, one may simply choose which fibration structure seems more convenient without loss of generality.

Definition 1: A purely wrinkled fibration is a smooth map from a 4-manifold to a 2-manifold whose critical locus consists of indefinite folds and indefinite cusps. A simplified purely wrinkled fibration is a purely wrinkled fibration $f\colon M \to S^2$ whose critical locus is a single circle on which f is injective.

Surface Diagrams

By corollary 1 of ref. 13, every broken Lefschetz fibration from a smooth, closed oriented 4-manifold M to the two-sphere can be modified by a (possibly long) sequence of moves (which are chosen from a short list initially appearing in ref. 4) into a simplified purely wrinkled fibration (in fact, the proof of that corollary implies this modification can be done for *any* map $M \to S^2$). Such a map has an orientable genus g surface as regular fiber over one of the disks that comprise $S^2 \setminus f(\mathrm{crit} f)$, and the generic fiber over the other disk has genus $g-1$; choosing a regular value p in the higher-genus side and reference arcs from p to the various indefinite fold arcs, one obtains a collection of simple closed curves in Σ_g by recording the round vanishing cycles in a counterclockwise direction going around the cusped critical circle. For this reason, the curves are relatively indexed by $\mathbb{Z}/k\mathbb{Z}$, where k is the number of fold arcs.

Definition 2: Assuming $g \geq 3$, a surface diagram (Σ_g,Γ) of M is the higher-genus fiber Σ_g, decorated with the relatively $\mathbb{Z}/k\mathbb{Z}$-indexed collection $\Gamma = (\gamma_1,\ldots,\gamma_k)$ of round vanishing cycles.

Remark 1: The requirement that $g \geq 3$ (which can always be satisfied by applying the stabilization deformation discussed below) is necessary for the following reason: After forming the fibration consisting of the preimage of a neighborhood of the critical image, if $g = 1$ or $g = 2$ there are various ways to close off the higher- and lower-genus sides with a copies of (fiber) $\times D^2$, according to the elements of $\pi_1(\mathrm{diff}\ S^2) = \mathbb{Z}_2$ and $\pi_1(\mathrm{diff}\ T^2) = \mathbb{Z}^2$, where $\mathrm{diff}(\Sigma)$ is the diffeomorphism group of Σ (see refs. 1 and 3 for explicit examples). Because $\mathrm{diff}(\Sigma_g)$ is simply connected for

$g \geq 2$, a surface diagram as defined specifies a 4-manifold up to diffeomorphism.

Remark 2: The local model for the cusp requires the two round vanishing cycles to transversely intersect at a unique point in the fiber; thus consecutive elements of Γ exhibit the same behavior. We call this requirement the intersection condition for surface diagrams, or simply the intersection condition when context makes it clear.

Moves on Surface Diagrams

This section describes discrete moves that may be used to modify a surface diagram while preserving the underlying smooth 4-manifold. Like the moves from handlebody theory, they are obtained as the endpoints of certain homotopies of the underlying fibration map. To keep the distinction clear, the terms handleslide, multislide, and stabilization will always refer to the move on surface diagrams, whereas the terms handleslide deformation, etc. will refer to the corresponding modifications of fibration maps, which may sometimes be performed on individual circles when the critical locus is not connected.

Stabilization. This move is a lightly disguised generalization of a homotopy that first appeared in figure 5 of ref. 3 and figure 11 of ref. 4. An example of how it affects a surface diagram is shown in Fig. 2. On the left of Fig. 2 is a small neighborhood νp of a point p of a circle c in a surface diagram (Σ_g,Γ). Stabilization results in a diagram $(\Sigma_{g+1} = \Sigma_g \#_{\partial \nu p} T^2, \Gamma')$, with Γ' obtained as follows. First note that, without loss of generality, $\Gamma \setminus c$ is disjoint from what appears in Fig. 2, and so it is unambiguous to say it is preserved under stabilization. Then $c \setminus \nu p$ patches in smoothly with one of the lower curves in the right of Fig. 2. The next curve in the sequence is either one of the parallel circles, followed by the circle at the very top of the torus. The sequence continues with the other one of the parallel circles, and finally a parallel copy of c patches in with the other curve at the bottom of the torus. The list of vanishing cycles then resumes as it did for Γ. Thus a stabilization at $p \in c$ could be said to insert four curves into Γ along with a torus connect summand into Σ. Fig. 3 depicts a base diagram for part of the stabilization deformation. Importantly, it is not straightforward to pin down the identification between the fibers above disjoint regions like in Fig. 3: In that figure, the vanishing cycles are drawn as they might appear once the intersection points are canceled.

In Fig. 3, two *flipping moves* from ref. 4 have been applied to the same fold arc. For a single flip, there is a local parameterization of the fiber such that the vanishing cycles appear in a standard way as in figure 5 of ref. 4 (the twice-punctured torus fiber in that figure is obtained from Fig. 2 by attaching a two-dimensional one-handle containing the rest of the two parallel vanishing cycles not fully depicted). However, there is no reason to expect that two flipping moves appear in this fashion, or that either should be required to appear in that standard way: Following the constraints given by the intersection condition and the local model for the flipping move, the variety in how Fig. 3 can appear is limited to allowing the vanishing cycles for the fold arcs at the tops of the two triangles to vary by positive or negative Dehn twists along the vanishing cycles for the central fold arc that runs between the two triangles; examples are shown in the figure. The stabilization deformation then continues as in refs. 3 and 4, canceling the two intersection points by a Reidemeister type-two move between the central fold arc and the critical arc connecting the two ends in Fig. 3, resulting in a simplified purely wrinkled fibration whose vanishing cycles can be deduced with little difficulty. The Reidemeister type-two move requires the two-sphere to be the base of the fibration to allow repeated stabilization.

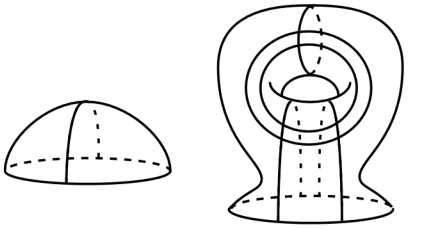

Fig. 2. An example of stabilizing a surface diagram.

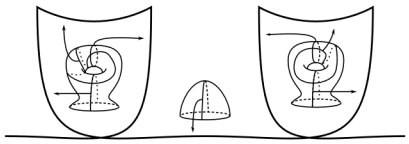

Fig. 3. The stabilization deformation involves two flipping moves that occur on the same fold arc. The disk in the left side of Fig. 2 is highlighted in the middle fiber.

One special case of stabilization is available to surface diagrams that come from surface bundles over the sphere—that is, blank surface diagrams. Performing a birth move in this case increases the genus of the surface diagram by one and introduces two simple closed curves whose only requirement is that they intersect at a unique point.

Handleslide. The handleslide is a modification whose appearance is formally like the one for Heegaard diagrams of 3-manifolds: In fact, the handleslide deformation is a one-parameter family of such moves, performed along a chosen fold arc. For a good description of the three-dimensional handleslide, see ref. 2. Two ways in which handleslides are different for surface diagrams is that we have not chosen a partition of Γ into sets of pairwise disjoint circles (so there is not immediately a distinguished collection of circles over which one may slide a given circle), and there is no linear independence requirement for the elements of Γ (so one might consider sliding a circle over another that happens to lie in the same isotopy class, resulting in a violation of the intersection condition). These considerations lead to additional assumptions as follows. Within the fibration underlying a surface diagram, denote four distinct components of the fold locus by A, B, C, D (with A, B, C consecutive), and label their vanishing cycles a, b, c, d. Then the requirement is that d is disjoint from each of a, b, and c [note this requirement implies $[a]$ and $[d]$ are linearly independent in $H_1(\Sigma)$ because of the intersection condition for a, b, c]. The handleslide then consists of replacing b with any simple closed curve b' that satisfies the intersection condition with its neighbors a and c, and such that the set of circles $\{b,b',d\}$ bounds an embedded thrice-punctured sphere $S \subset \Sigma$.

The modification comes from the following deformation. First, in base diagrams, B (and a small amount of A and C) moves across the higher-genus region of the fibration into the lower-genus side of D in a Reidemeister type-two move as depicted in Fig. 4, which is possible by the disjointness assumption. Along the higher-genus side of A, Σ has experienced a surgery along d so that a becomes able to move by isotopy over either of the two points (depicted in the figure) that become identified as one traces a reference arc to the lower-genus side of D; in other words, the boundary component d of S has been capped off in this region. The last step is to cancel the two intersection points by the reverse Reidemeister type-two move in which B moves back the way it came across D. The vanishing cycles have now changed by replacing b with a band sum of b and d, giving the embedding of S.

Multislide. Independently found by Denis Auroux and Rob Kirby, this move comes from a deformation in which the critical locus becomes momentarily disconnected. To perform the multislide, one first finds a nonconsecutive pair of vanishing cycles that in-

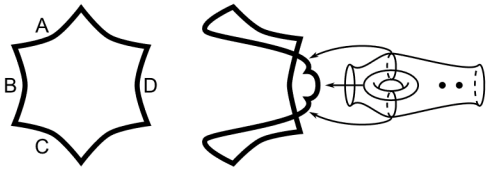

Fig. 4. Base diagrams for part of the handleslide deformation. The initial surface diagram is obtained as the preimage of a point in the center of the circle on the left, decorated with vanishing cycles obtained by following radial reference arcs.

tersect transversely at a unique point in Σ, say γ_1 and γ_n. One also chooses one of the subsets $\{\gamma_2,\ldots,\gamma_{n-1}\}$ or $\{\gamma_{n+1},\ldots,\gamma_k\}$ on which to perform the move: choose the first subset for expediency. A sufficiently small tubular neighborhood of the chosen pair in Σ is a punctured torus, and one may replace that torus momentarily with a disk that has marked points on its boundary according to the places where $\gamma_1,\ldots,\gamma_k$ may have entered and exited the torus, resulting in a surface Σ' whose genus is one less than that of Σ, decorated with the resulting collection of curves $\gamma'_1,\ldots,\gamma'_k$ (there will be one pair of marked points for each intersection between $\gamma_1,\ldots,\gamma_k$ and the chosen pair). One may then perform a one-parameter family of diffeomorphisms of $(\Sigma',\gamma'_2,\ldots,\gamma'_{n-1})$ in which the disk travels along an arbitrary circle, returning to where it started and dragging the chosen subset $\gamma'_2,\ldots,\gamma'_{n-1}$ along with it (but leaving all the other vanishing cycles $\gamma_n,\ldots,\gamma_1$ unchanged). A choice of framing allows those elements of $\{\gamma'_2,\ldots,\gamma'_{n-1}\}$ with marked points to be affected by a power of a positive or negative Dehn twist along the boundary of the disk. After performing this modification of the chosen subset, one reattaches the punctured torus according to the marked points. To explain the terminology, it is as if a handleslide has been performed in which a collection of vanishing cycles slides over the chosen pair, which is not to say the multislide is a sequence of handleslides: The multislide can change the free homotopy class of the underlying fibration's critical circle, something the previous two moves cannot achieve.

The multislide deformation is depicted in Fig. 5. To begin, choose a pair of fold arcs whose vanishing cycles happen to intersect transversely at a unique point in the fiber. On the left side of Fig. 5, a vertical arc joins the chosen pair, signifying a move that results in the middle figure (this move is called a merge in ref. 4 and a cancellation in ref. 14). The inside of each of the two circles now has Σ as its generic fiber, with vanishing cycles obtained from Γ by deleting those whose fold arcs were "pinched off" into the other circle by the merging move (this is where the partition

$$\Gamma \setminus \{\gamma_1,\gamma_k\} = \{\gamma_2,\ldots,\gamma_{n-1}\}\cup\{\gamma_{n+1},\ldots,\gamma_k\}$$

comes from). The deformation concludes with a move in which the two circles reunite along the two newly formed cusps. To explain the modification of surface diagrams, consider the deformation as a map $[0,1]\times M \to [0,1]\times S^2$ that restricts to the identity map in the first factors. The critical image is a properly embedded twice-punctured torus in $[0,1]\times S^2$. If one chooses two reference points on the left side of the figure such that one splits into each circle, initially their base diagrams are isotopic. However, the identification between them is modified by the time the two circles rejoin: Note that the cusps that form and then disappear trace out a circle in $[0,1]\times M$. Projecting out the homotopy parameter yields a circle $\alpha \subset M$, and without loss of generality one of the pair of cusps, say the right, remains stationary throughout its life, whereas the other traces out α as the homotopy progresses (the resulting surface diagram will then be the one obtained using a reference point that stays in the right circle through the deformation). To say it a different way, the horizontal arc in the middle of Fig. 5 can be taken as the image of that part of α over which the left cusp will travel. This so-called joining curve is framed, and everywhere transverse to the fiber. The fibers containing points on its interior serve as Σ', with the disk mentioned above coming from a fiberwise neighborhood of the joining curve. The circle α projects to the circle in Σ' along which this disk travels, inducing the above-mentioned isotopy of $\{\gamma'_2,\ldots,\gamma'_{n-1}\}$. In this way, the choice of α induces an element of the mapping class group of Σ that only applies to those vanishing cycles coming from the left circle.

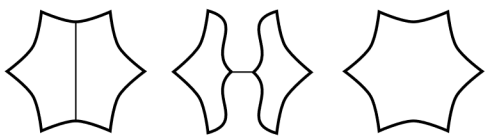

Fig. 5. The multislide deformation. The initial fibrations for this and Fig. 4 have six cusps for no particular reason.

Shift. This move embodies the possible variations on the ordering of the vanishing cycles in a surface diagram. In base diagrams, the deformation is similar to that of the multislide in Fig. 5, but instead of reuniting the two circles at the two newly formed cusps, one of those cusps instead meets with a cusp that is adjacent to the other.

To understand how this deformation affects a surface diagram, it is useful to consider what we will call a "surgered surface diagram." This viewpoint is useful for understanding all the moves, but in the interest of brevity, we illustrate it only for shifting. In the initial simplified purely wrinkled fibration, consider a reference fiber Σ_{g-1} over a point just to the lower-genus side of a fold arc γ, along with a short reference path across γ into its higher-genus side. As one traces fibers above this path, two points p, p' become identified in a surgery that increases the genus of the fiber by one, as in Fig. 1*A*. Then the endpoint of this path gives a reference fiber Σ_g to which one can add the vanishing cycles for folds bounding that higher-genus region. Pulling this picture back across γ, all the vanishing cycles descend to circles in Σ_{g-1} except those that intersect the vanishing cycle of γ; these instead appear as vanishing arcs whose endpoints are p and p'. The ends of these arcs come equipped with a bijection β between those at p and those at p' by the way they pair up on either side of the vanishing cycle of γ in Σ_g; for this reason, the union of vanishing arcs obtained by picking a point on one vanishing arc, following it to one end e, continuing at $\beta(e)$, and on until returning to the chosen point will be called a vanishing cycle just like the other simple closed curves. In this way, the base diagram can be recovered from a reference fiber in the lower-genus region, along with a chosen path into the higher-genus region.

Taking a family of such reference fibers and paths along the critical circle of the fibration yields a one-parameter family of such diagrams, and this paragraph describes how such a family evolves when a reference path passes a cusp (it is helpful to imagine a family of horizontal arcs in Fig. 1*B*). As the family of paths approaches a cusp, there is a vanishing arc ν, coming from the vanishing cycle just past the cusp, whose ends correspond under β (thus ν is itself a vanishing cycle). The points p and p' travel along ν as it shrinks to a point where p and p' momentarily meet, so that the diagram whose path intersects the cusp itself has only one distinguished point. Passing the cusp, p and p' separate again; now they form the pair of points whose surgery has belt circle ν. Those vanishing cycles intersecting ν in Σ_g form the new collection of vanishing arcs, whereas those ends that came from vanishing cycles disjoint from ν, brought together with p and p', disengage from p and p' without reseparating. With this understood, it becomes clear that the surgered surface diagrams coming from reference paths on either side of a cusp are identical up to isotopy.

For the shift deformation, we choose a reference point in the lower-genus region and a fold arc γ that takes part in the initial merge or cancellation. Also, choose two reference paths from